PHOTODISINTEGRATION OF Li^7

L. A. KUL'CHITSKIĬ and Yu. M. VOLKOV

A. F. Ioffe Physico-technical Institute, Academy of Sciences, U.S.S.R.

Submitted to JETP editor November 10, 1962

J. Exptl. Theoret. Phys. (U.S.S.R.) 44, 1153-1159 (April, 1963)

The energy spectra and angular distributions of protons and tritons produced in the photodisintegration of Li^7 are investigated. In the energy spectrum of phototritons produced at $E_{\gamma max} = 30$ MeV the observed groups correspond to excitation energies of 14.1, 16.2, 18.0, 19.6, 21.5, 23.5, and 25.3 MeV. In most of the energy ranges the triton angular distributions have the form $\sim \sin^2\vartheta$. Pronounced peaks have also been found in the Li^7 photoproton spectra. However, for $E_{\gamma max} = 25$ and 30 MeV the bulk of the observed protons are associated with transitions to excited states of the He^6 nucleus.

INTRODUCTION

It has been established that the probability of the reaction $Li^7(\gamma, t)He^4$ is comparable to that of the (γ, n) and (γ, p) reactions in the photodisintegration of Li^7. The energy spectra of the tritons have revealed sharply defined groups, leading to the hypothesis that at relatively low excitation energies the reaction occurs via a compound nucleus [1,2]. The angular distributions, which are close to $1 + \sin^2\vartheta$ for the principal triton groups, represent dipole transitions to excited Li states with spin $^5/_2$.

For $Li^7(\gamma, t)He^4$, Czyz [3] has considered theoretically the direct photodisintegration mechanism of Li^7 as a system consisting of an α particle and a triton in the $P_{3/2}$ state. In this model, the triton angular distributions should have the form $1 + 1.5 \sin^2\vartheta$.

In [4] we obtained an angular distribution of 7.5—15-MeV tritons represented by $a + b\sin^2\vartheta$ with $b/a = 2.5$. It is difficult to reconcile this distribution with the aforementioned hypotheses regarding the mechanism of $Li^7(\gamma, t)He^4$.

Shardonov and Shevchenko [5] have obtained the energy spectrum and angular distribution of protons from the photodisintegration of Li^7 ($E_{\gamma max} = 17.5$ MeV). The energy groups in the proton spectrum were regarded as corresponding to excited Li^7 levels.

In the present work we have investigated the energy spectra and angular distributions of protons and tritons produced in the photodisintegration of Li^7 at different values of $E_{\gamma max}$.

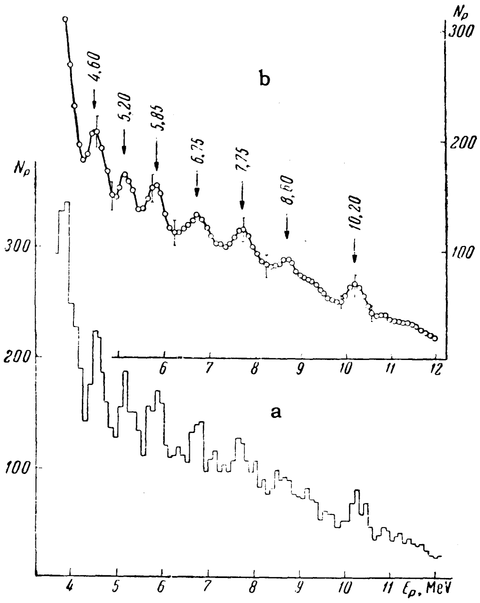

FIG. 1

EXPERIMENTAL PROCEDURE

The experimental technique and method of identifying and measuring the energies of charged particles produced in photodisintegration are similar to those described in [4] except for some changes in the apparatus. A lithium target 8 mg/cm² thick was placed in a vacuum chamber in conjunction with two identical counter telescopes. The head counters of the telescopes, giving pulses proportional to the energy loss $\Delta E \sim dE/dx$, were proportional counters filled with argon and a small admixture of methane; this made possible registration of photoreaction products having somewhat lower energies, and also enhanced the energy (ΔE) resolution of the telescopes.

In order to reduce the distortions of pulses

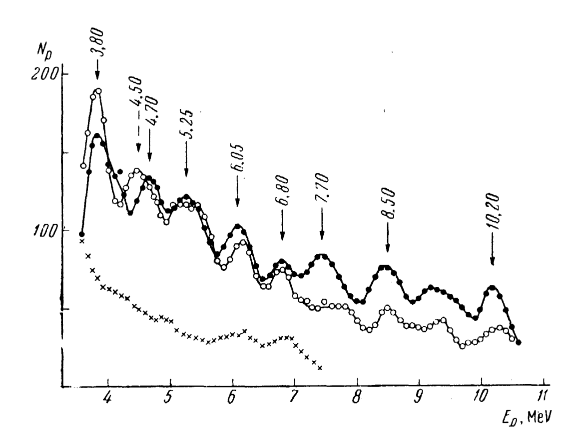

FIG. 2. Smoothed energy spectra of photoprotons from Li^7 for $E_{\gamma\,max}$ = 20 MeV (×), 25 MeV (o), and 30 MeV (•). Ordinates represent the proton yield (in arbitrary units) relative to an identical total γ-ray energy. The arrows indicate the spectral peaks.

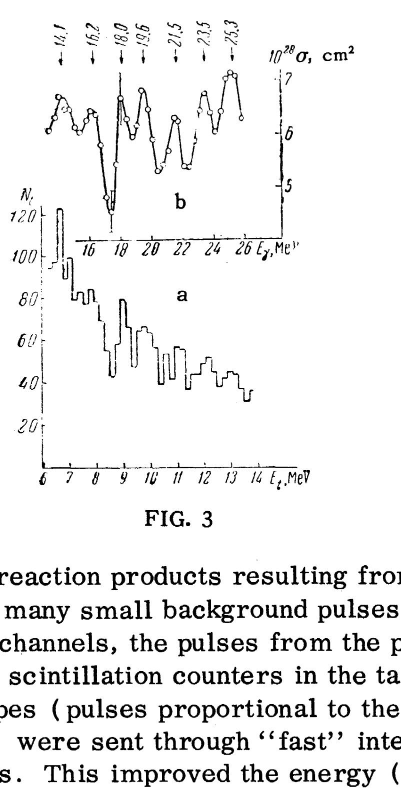

FIG. 3

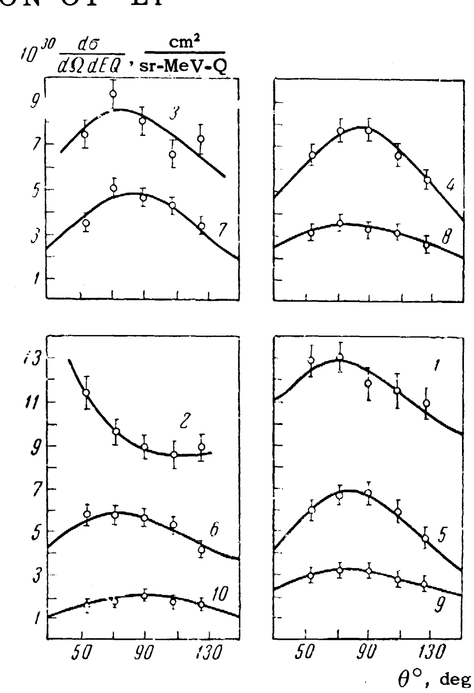

FIG. 4. Angular distributions of protons from Li^7 photodisintegration at $E_{\gamma\,max}$ = 30 MeV for different energy intervals: 1 – 3.8–4.2 MeV; 2 – 4.5–4.9 MeV; 3 – 5.2–5.7 MeV; 4 – 5.8–6.4 MeV; 5 – 6.6–7.2 MeV; 6 – 7.7–8.3 MeV; 7 – 8.6–9.2 MeV; 8 – 9.4–10.8 MeV; 9 – 10.2–10.8 MeV; 10 – 11.0–12.1 MeV. The smooth curves were obtained by least squares using the formula $a + b\sin^2\vartheta(1 + \gamma\cos\vartheta)^2$. Ordinates represent the differential cross section per effective quantum.

representing reaction products resulting from the integration of many small background pulses in the amplification channels, the pulses from the photomultipliers of scintillation counters in the tail ends of the telescopes (pulses proportional to the particle energy E) were sent through "fast" integral discriminators. This improved the energy (E) resolution of the telescopes.

In these experiments we did not employ special circuits to stabilize the amplification of the scintillation counters.

EXPERIMENTAL RESULTS

Figure 1a shows the combined energy spectrum of protons emitted in the photodisintegration of Li^7 by bremsstrahlung having $E_{\gamma max}$ = 30 MeV at the angles 54°, 72°, 90°, 108°, and 126°. In Fig. 1b the same spectrum has been smoothed out; the arrows point to peaks appearing in all the proton spectra registered by both telescopes at the indicated angles.

Figure 2 shows the smoothed energy distributions of protons emitted in the photodisintegration of Li^7 for $E_{\gamma max}$ = 20, 25, and 30 MeV (ϑ = 90°).

Figure 3a shows the combined energy spectrum of tritons measured under the same conditions as the proton spectrum in Fig. 1. Fig. 3b shows the cross section curve for $Li^7(\gamma, t)He^4$ derived from the smoothed triton spectrum. The arrows indicate the peaks appearing in all measurements with both telescopes at the given angles.

The angular distributions of photoprotons and phototritons for different energy intervals are shown in Figs. 4 and 5. The angular distributions were approximated by an analytic expression of the form $a + b\sin^2\vartheta(1 + \gamma\cos\vartheta)^2$. The values of a/b and γ determined by least squares, for the proton and triton angular distributions in the separate energy intervals, are given in Tables I and II.

Table III gives the cross sections for the production of protons, deuterons, and tritons per effective quantum in the interval 4.8–7.8 MeV for different values of $E_{\gamma max}$ (ϑ = 90°). The data in Table III include only the statistical errors and the errors associated with inaccurate mass resolution of the particles in treating the data.

Table I

Proton energy interval, MeV	Proton angular distribution $a + b\sin^2\vartheta(1+\gamma\cos\vartheta)^2$ a/b	γ	Proton energy interval, MeV	Proton angular distribution $a + b\sin^2\vartheta(1+\gamma\cos\vartheta)^2$ a/b	γ
3,8—4,2	2.8±0.5	0.4±0.1	7,7—8,3	1,43±0,30	0,35±0,1
4,5—4,9	—5.0±0.7	—	8,6—9,2	0,28±0,04	0,08±0,1
5,2—5,7	3.2±0,7	0.25±0.1	9,4—10,0	1,35±0,25	0,24±0,1
5,8—6,4	0.57±0,07	0.135±0.1	10,2—10,8	1,28±0,25	0,23±0,1
6.6—7,2	0.61±0.08	0.20±0.1	11,0—12,1	0.69±0.15	0,0±0,1

Table II

Triton energy interval, MeV	Triton angular distribution $a + b\sin^2\vartheta(1+\gamma\cos\vartheta)^2$ a/b	γ
6,7—7,2	—0,07±0,12	—0,05±0,05
7,4—8,4	0,15±0,15	—0,2±0,1
8,6—11,4	0,025±0,08	—0,05±0,05
11,8—12,6	0,50±0,15	—0,3±0,1
6,7—12,6	0,1±0,08	—0,12±0,1
7,5—15 [4]	0,4±0,07	—

Table III

Particle	$10^{30}\frac{d\sigma}{d\Omega\, dE\, Q}$, $\frac{cm^2}{sr\text{-}MeV\text{-}Q}$ $E_{\gamma\,max}$ = 20 MeV	$E_{\gamma\,max}$ = 25 MeV	$E_{\gamma\,max}$ = 30 MeV
p	2,7±0.2	8.6±0.4	12,7±1,2
d	0,11±0,03	0,40±0.12	0.60±0.3
t	1,36±0,24	1,36±0,12	1,56±0.2

Table IV

E_t, MeV	E_γ, MeV	Energy level of Li^7 [6]	E_t, MeV	E_γ, MeV	Energy level of Li^7 [6]
6,6±0.2	14,1±0,3	14,0	10,9±0.2	(21,5±0,3)*	(21,5)
7,8±0.2	16,2±0.3	16,2	12,1±0,2	(23,5±0.3)	(23,5)
9.0±0,2	18,0±0,3	17,5	13,0±0,2	(25,3±0,3)	—
9,8±0.2	19,6±0,3	—			

*Less reliable values are given in parentheses.

DISCUSSION OF RESULTS

The peaks of the cross section for $Li^7(\gamma, t)He^4$, denoted by arrows in Fig. 3, were compared with the excited levels of Li^7 in [6]. Table IV shows that there is good agreement for the levels at 14.1, 16.2, 21.5, and 23.5 MeV. This can indicate that the reaction $Li^7(\gamma, t)He^4$ involves the formation of a compound nucleus. Levels corresponding to the peaks at 19.6 and 25.3 MeV still apparently have not been observed.

The angular distributions of tritons from $Li^7(\gamma, t)He^4$, calculated from the theory of resonance γ-ray absorption with compound-nucleus formation, are given in [1,2]. None of these distributions agrees with the angular distributions of the form $\sim\sin^2\vartheta$ in the present work (Table II). Tritons associated with transitions to excited Li^7 states having a specified spin J can be emitted with different orbital momenta l; therefore the angular distributions should have the form [7]

$$d\sigma(\vartheta)/d\Omega \sim \sum_{ll'L} \mathrm{Re}\{R_{l'}^{J*}R_l^J\}\, Q_L^{ll'} P_L(\cos\vartheta)$$

($R_{l'}^J$ and R_l^J are the matrix elements of the operator $\hat{R} = i\hat{S} - \hat{1}$, where S is the scattering matrix, $\hat{1}$ is the unit matrix, $Q_L^{ll'}$ are numerical coefficients depending on l and L, and P_L are Legendre polynomials), if we do not consider the possible interference of the absorption of γ quanta of different multipolarities. At the present time it is impossible to calculate theoretically the matrix elements R_l^J determined by the nuclear structure. We cannot exclude the possibility that in the reaction under consideration the relations between the matrix elements will lead to the vanishing of the isotropic part of the angular distribution. However,

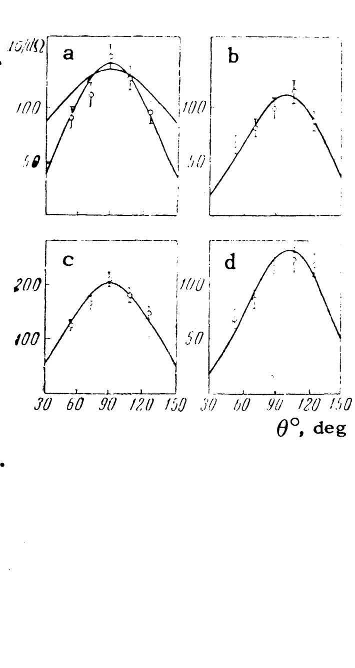

FIG. 5. Angular distributions of phototritons from $Li^7(\gamma, t)He^4$. Ordinates represent the reaction cross section in arbitrary units at $E_{\gamma\,max}$ = 30 MeV in different energy intervals: a – 6.7–7.2 MeV; b – 7.4–8.4 MeV; c – 8.6–11.4 MeV; d – 11.8–12.6 MeV. The continuous curves for the first energy interval were obtained using the formulas $\sin^2\vartheta$ and $1 + \sin^2\vartheta$; for the other intervals the curves were obtained by least squares from the formula $a + b\sin^2\vartheta(1+\gamma\cos\vartheta)^2$.

Table V

Proton group energy, MeV	% of protons accompanying transitions to second and higher excited states of He^6		Proton group energy, MeV	% of protons accompanying transitions to second and higher excited states of He^6	
	$E_{\gamma max}$ = 25 MeV	$E_{\gamma max}$ = 30 MeV		$E_{\gamma max}$ = 25 MeV	$E_{\gamma max}$ = 30 MeV
3.8	50*	50*	6.80	28	40
4.6	90	90	7.70	30	50
5.25	75	85	8.60	45	85
5.85	34	60	10.20	0	45

*% of protons accompanying transitions to the third and higher excited states of He^6.

it may appear surprising that this shape of the angular distribution is observed for a broad energy interval containing several excited levels.

In [3] the total integral and differential cross sections for $Li^7(\gamma, t)He^4$ were calculated on the two-particle model of Li^7, in which it is assumed that Li^7 consists of an α particle and a triton in the $P_{3/2}$ state. The general formula representing the differential cross section for Li^7 disintegration into an α particle and a triton through the dipole absorption of γ quanta is

$$\sigma(\vartheta) = \frac{\sigma_{PD}}{100\pi}\left(\frac{25}{2} + \frac{75}{4}\sin^2\vartheta\right) + \frac{1}{4\pi}\sigma_{PS} \mp \frac{1}{4\pi}\sqrt{2\sigma_{PS}\sigma_{PD}}\cos(\delta_2 - \delta_0)\left(\frac{3}{2}\sin^2\vartheta - 1\right);$$

σ_{PD} and σ_{PS} were calculated assuming square-well potentials of different depths for states with different orbital momenta (V_S, V_P, and V_D for S, P, and D states, respectively). V_S and V_D were selected for agreement with the experimental angular distributions of the form $1 + 1.5 \sin^2\vartheta$ given in [1] for 4.7-MeV γ rays. On this model V_S and V_D could probably be selected to make the isotropic part of the angular distribution so small as to produce agreement with the results of the present work. It must be remembered, however, that the calculations represent a very rough approximation.

In order to account for the experimental angular distributions of phototritons and the structure of the spectra it must evidently be assumed that both of the discussed processes of phototriton production actually take place.

The identification of groups in the photoproton spectra is hindered by possible transitions to different excited states of the final He^6 nucleus (1.71, 3.4, 6.0, and 9.3 MeV).[6] The photoproton spectra obtained for three values of $E_{\gamma max}$ (20, 25, and 30 MeV) permit only tentative conclusions regarding the probabilities of transitions to different excited states for separate groups.

Table V gives the probabilities of transitions to the second and higher excited states of He^6, for the different proton groups, with $E_{\gamma max}$ = 25 and 30 MeV. These data suggest that the bulk of the protons produced through photodisintegration by the given bremsstrahlung spectra are associated with transitions leaving the residual nucleus in an excited state.

The angular distributions of photoprotons in the separate groups differ strongly from each other with respect to the ratio of the coefficients a and b (see Table I), and for most of the groups are not in disagreement with the distributions based on the compound-nucleus model. However, the existence of angular distributions having the form $1 + 1.5 \sin^2\vartheta$ for three-proton energy intervals indicates that direct photoproton emission is also possible.

In conclusion the authors wish to thank G. M. Shklyarevskiĭ for discussions of the results, and also the cyclotron crew.

[1] Erdös, Stoll, and Wächter, Nuovo cimento 12, 639 (1954).

[2] V. G. Shevchenko and B. A. Yur'ev, Izv. AN SSSR, Ser. Fiz. 25, 1269 (1961), Columbia Tech. Transl. p. 1280.

[3] W. Czyż, Acta Phys. Polonica 15, 129 (1956).

[4] Yu. M. Volkov and L. A. Kul'chitskiĭ, JETP 42, 108 (1962), Soviet Phys. JETP 15, 77 (1962).

[5] A. Kh. Shardanov and V. G. Shevchenko, JETP 42, 1438 (1962), Soviet Phys. JETP 15, 996 (1962).

[6] F. Ajzenberg-Selove and T. Lauritsen, Nuclear Phys. 11, 1 (1959).

[7] Baldin, Gol'danskiĭ, and Rozental', Kinematika yadernykh reaktsiĭ (Kinematics of Nuclear Reactions), Fizmatgiz, 1959.

Translated by I. Emin
190